Modern Environmental Science and Engineering (ISSN 2333-2581)
May 2020, Volume 6, No. 1, pp. 1218-1226
Doi: 10.15341/mese(2333-2581)/01.06.2020/009
Academic Star Publishing Company, 2020
www.academicstar.us

Synthesis and Photocatalytic Activity of Nano Eu_2O_3/TiO_2 in the Degradation of Methylene Blue in Aqueous Solution

Van Tien Mai, and Le Thi Hai Le

Hanoi University of Natural Resources and Environment, Vietnam

Abstract: Eu_2O_3/TiO_2 catalyst nanocomposite materials were synthesized from tetra-n-butyl orthotitanate, rare earth oxide Eu_2O_3 by a sol gel method, with a polyvinyl alcohol gel agent. Characteristic structures and properties were determined by infrared (IR) spectrometry, X-ray diffraction, a scanning electron microscope (SEM), and a transmission electron microscope (TEM). The composition and ingredients of Eu_2O_3/TiO_2 and the Ti/Eu ratio were shown in the XRD diagram and Energy Dispersive X-ray (EDX) fluorescence spectroscopy. The results of testing the photocatalytic properties of the material to treat methylene blue (MB) with a concentration of 20 ppm in water for processing efficiency reached over 92.7%. The obtained materials, namely photochemical catalyst materials, can be applied in the field of environmental treatment, especially photochemical catalytic decomposition catalysts in visible light to treat textile wastewater and organic pollutants in water, as well as bactericidal effects.

Key words: photocatalytic, oxide of Eu_2O_3, TiO_2, oxidation, methylene blue in aqueous solutions, wastewater

1. Introduction

TiO_2 nano is the most researeched material nowadays as it has low toxicity, is sustainable and is inexpensive. TiO_2 is a semiconductor with a band gap at 3.05 eV for rutile and 3.25 eV for anatase, therefore, it can perform photocatalytic reactions and be particularly observed as a photocatalyst in applications to disinfect and decompose sustainable organic compounds in water [1-4]. The photocatalytic capability of TiO_2 is represented by three effects: photocatalysed dehydration on TiO_2 electrodes, creating ultra-permeable surface and photocatalytic decomposition of organic matter under ultraviolet light $\lambda < 380$ nm. However, the amount of ultraviolet radiation (UV) in the solar spectrum to the earth surface is only 3.5-4%, so the use of this radiation source for environmental treatment with photocatalytic TiO_2 is limited [5, 6]. In order to extend the use of solar radiant energy even from the visible light region for photocatalytic reactions, the forbidden band of TiO_2 must be smaller [7-10, 16]. In order to achieve that goal, many research projects have denatured nanostructures of TiO_2 by introducing metal and non-metal ions to its surface or into its structure. At present, there are four directions for studying, including making and applying photocatalyst materials based on pure TiO_2, TiO_2 denatured by nonmetals, TiO_2 denatured by metals and by mixed oxides of metal or non-metal [11-15].

Rare-earth oxides are widely used for various applications such as optoelectronic devices, catalysts and electrochemical applications. Among rare-earth oxides, Eu_2O_3 is one of the most important because the Eu^{3+} ion has a maximum emission wavelength range of 610-612 nm. Currently mixed oxide systems, such as CeO_2, Nd_2O_3, Eu_2O_3, Y_2O_3, with titanium oxide is also an object of special interest to many scientists, due to

Corresponding author: Le Thi Hai Le, Ph.D.; research areas/interests: environmental monitoring and toxicology. E-mail: drlhaile@gmail.com.

their unique properties and applicability that individual oxides do not have. Many studies show that the combination of Eu_2O_3 and TiO_2 will form a photocatalytic material system with strong catalytic activity in the visible light area [20-24].

The manufacturing methods of materials in general and nanomaterials in particular, is very diverse. There are two approaches to synthesizing nanomaterials: the top-down and the bottom-up approach. The top-down approach uses physical methods such as condensation, from steam phase, fumigation, chemical deposition, etc., and the bottom-up approach is usually done by chemical pathways with co-precipitation, reduction, explosion, hot spray thermal decomposition, micelles, sol-gels, flocculation, and hydrothermal methods. The advantage of physical methods is the synthesis of large numbers of nanoparticles, but the uniform particle size is not high due to difficulty in controlling particle size. The advantage of the chemical method is that it is possible to control the particle size and obtain uniform nanoparticles [17-20].

In this study, we chose to synthesize Eu_2O_3/TiO_2 photo-catalytic catalyst composite materials by the sol gel method, because this is a simple method that is easy to implement. The sol gel burning process can produce nano oxide and mixed nano oxide crystals at a lower temperature in a short time and can reach the final product immediately without further processing, thus limiting the intermediate phase formation and secretion energy [29]. The effect of Eu/Ti doping ratio, heating temperature, solution pH and initial methylene blue (MB) concentration on the structure, morphology, composition and visible radiation absorption of Eu_2O_3/TiO_2 as well as the ability of MB photochemical decomposition photocatalytic will be discussed in this paper.

2. Experimental Section

2.1 Chemicals

All the reagents and chemicals were of analytical grade and used without further purification. Tetra-n-butyl orthotitanate ($C_{16}H_{36}O_4Ti$, Sigma-Aldrich, Germany), Eu_2O_3 (Merck Millipore, Germany), nitric acid (HNO_3, Merck), alcohol (C_2H_5OH, Merck), acetone ($C_3H_6O_2$ Merck), PVA-205 (Mw: 10.000 g/mol, Chiyoda-Ku, Tokyo, Japan), and original standard methylene blue (MB) solution (1000 ppm, Merck).

2.2 Equipment

The devices used for research include:

- Optical absorption meter Dr 500 (Hach, USA).
- X-ray analyzer, EDX-D8 Advance (Bruker, Germany);
- TEM-Tecnai G20 capture device (Shimadzu, Japan);
- Infrared (IR) spectrum is measured on a Bruker-Tensor machine (Bruker, Germany);
- Photographing SEM Jeol JMS 6490 electron microscope (Edax, Japan).

2.3 Synthesis of a Photocatalytic System Based on Nano Eu_2O_3/TiO_2

2.3.1 Process Protocols

The Eu_2O_3/TiO_2 photocatalytic nanomaterials were prepared by a sol-gel method using $Ti(OC_4H_9)_4$ and Eu_2O_3 as the raw material source. The synthesis process is as follows:

First, the oxide of Eu_2O_3 was transfered to the form of $Eu(NO_3)_3$ by completely dissolving Eu_2O_3 with an excess of HNO_3 (2N). The excess acid was evaporated by boiling on a water bath at 80°C÷95°C until becoming a damp salt, distilled water was added and the evaporating excess acid was continued. This process was repeated three to five times to produce pure salt crystals of $Eu(NO_3)_3$, which was followed by drying at 105°C to a constant weight.

Next, the pre-calculated masses of $Ti(OC_4H_9)_4$; $Eu(NO_3)_3$ and PVA were introduced into the reactor. The pH was adjusted to about 4 by HNO_3 (2%). Gel forming agitation was performed and aging of $Ti(OH)_4$-$Eu(NO_3)_3$ gel was carried out by PVA with the content of 10%, at 100°C for 2 hours. The formed gel

was dried at 105°C for 8 hours until a dry light-pink white powder was obtained. The nanomaterial samples of Eu_2O_3/TiO_2 mixed oxides were prepared with different TiO_2/Eu_2O_3 ratios and calcinations at 450°C to 550°C for 3 hours [1, 13, 22, 24], then analyzed by XRD, SEM, IR, and TEM to determine any changes in the crystal structure, phase composition, and average particle size of the materials. The EDX spectra of Eu_2O_3/TiO_2 samples were recorded to determine the presence and the content of the material components.

2.4 Oxidative Photodesulfurization of Methylene Blue

Evaluation of photocatalytic activity of Eu_2O_3/TiO_2 on a static model of a wastewater sample with 20 ppm MB, was carried out as follows: 100 mL of methylene blue solution was placed in a 250 ml beaker containing 0.05 g catalyst. The suspension was stirred in the dark or was illuminated with two 15 W UV lamps (UV light) or a 165 W tungsten lamp (visible light) at various temperatures and times. After a certain reaction time, a small amount of each product was removed, centrifuged, and analyzed by molecular absorption spectroscopy at 660 nm wavelength. The percentage of degradation of MB (η) was calculated according to the initial, C_o (ppm), and the final, C (ppm), concentrations of MB in the solution following this equation:

$$\eta = 100 \times (C_o - C)/C_o$$

2.5 The Effect of Eu_2O_3/TiO_2 Ratio on the Photocatalytic Activity of MB

50 mg of Eu_2O_3/TiO_2 catalyst samples was weighed exactly with different Eu_2O_3:TiO_2 ratios of Eu_2O_3/TiO_2**,** 0/1, 1/5, 1/10, 1/15 and 1/20, into conical flasks containing 100 ml of MB 20 ppm. Reaction time was 2 hours, the solution was stirred continuously at 70°C using a tungsten lamp 20 cm away from the surface of the solution to light up the reaction solution surface. At the end of the experiment, analytical centrifuging determined the concentration of MB by measuring the absorbance at 660 nm.

2.6 The Effect of Burning Temperature, When Manufacturing Catalysts, on the Ability to Decompose Methylene Blue

The catalytic synthesis process was performed as above. The burning temperature was selected to make the mixture of catalyst materials according to the document [2, 3]. The temperature was selected at 4500°C, 5000°C, 5500°C, 6000°C, after a 3-hour sample heating time, and the Eu_2O_3/TiO_2 ratio *i* was 1/15.

2.7 The Effect of pH on the Decomposition of the MB Catalyst

MB digestion reaction was performed by taking exactly 50 mg of an Eu_2O_3/TiO_2 catalyst sample with an Eu_2O_3:TiO_2 ratio of 1/15 into conical flasks containing 100ml of MB 20 ppm. The reaction time was 2 hours, stirring the solution continuously at 70°C, under visible light conditions. The pH conditions varied from 2 to 12 when adjusted with HNO_3 2% and NaOH 5% solutions. At the end of the reaction, centrifuge sampling was used to remove the solids and take optical measurements to determine the concentration of MB.

2.8 The Effect of Temperature on Decomposed of MB

An experimental survey of the effect of the reaction mixture temperature on the photocatalytic oxidation of MB was carried out by selecting 3 temperature zones, 30°C, 50°C and 70°C, then proceeding similarly as above. The reaction mixture was carried out under visible light conditions, the reaction time was in 2 hours, stirring the solution continuously. The reaction temperature was stabilized, maintained by a thermal stabilizer. The Eu_2O_3/TiO_2 nano photocatalyst sample with Eu_2O_3:TiO_2 ratio of 1/15 was used, and the initial MB concentration was 20 ppm.

2.9 Evaluation of the Photocatalytic Activity of Eu_2O_3/TiO_2 Nanomaterials Under Different Lighting Conditions (Natural Light, No Light and UV Light)

Photocatalytic activity of Eu_2O_3/TiO_2 mixed oxide with Eu_2O_3:TiO_2 = 1/15 ratio was performed under the conditions of UV light, visible light and no light; UV light using 2 15 W UV lamps, visible light with a 165 W tungsten lamp and no light by using aluminum foil to seal the reaction vessel. The MB decomposition test was performed at 70°C, the concentration of MB was 20 ppm, and pH = 4. After a certain duration time, the centrifuge sample was measured at the absorbance of 660 nm to determine the remaining MB concentration in the solution.

2.10 Determination of Photocatalytic Reaction Kinetics

The Langmuir-Hinshelwood model was applied to test the photocatalytic reaction kinetics. The Dynamic equations applied:

$$Ln\ (C_o/C_{t)} = k_{app}.t$$

Where: C_o and C_t are the reactant concentrations at times t = 0 and t = t, kapp is the reaction rate constant.

3. Results and Discussion

3.1 Characteristics of Photocatalyst Based on Eu_2O_3/TiO_2

3.1.1 IR spectra of Eu_2O_3, TiO_2 and Eu_2O_3/TiO_2

Infrared spectra of Eu_3O_2 (Fig. 1) showed peaks of oscillation at: 1486.83 cm^{-1}, 1384.7 cm^{-1}, 535.45 cm^{-1} and 477.87 cm^{-1}. Infrared spectra of TiO_2 showed peaks of oscillation of the TiO_2 molecule at: 1631.3 cm^{-1}, 979.82 cm^{-1} and 751.38 cm^{-1}. Infrared spectra of Eu_2O_3/TiO_2 had peaks at: 1631.3 cm^{-1}, 979.82 cm^{-1}, and 750.38 $cm^{-1,}$ characteristic oscillations of the links in TiO_2. The peaks were at 1486.83 cm^{-1}, 1384.7 cm^{-1}, 535.45 cm^{-1}, and 477.87 cm^{-1}, characteristic of the oscillation of Eu_2O_3 links with the same width with a difference of < 50 cm^{-1}: 1487cm^{-1}, 93 cm^{-1}, 1388 cm^{-1}, 509.79 cm^{-1}, and 464.07 cm^{-1}. That proves that the synthesis of Eu_2O_3/TiO_2 materials was successful.

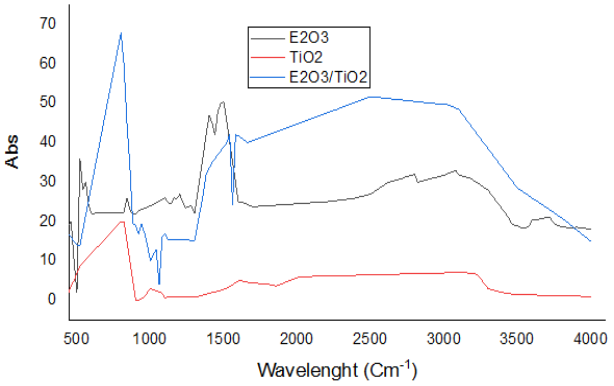

Fig. 1 IR spectra of Eu_2O_3, TiO_2 and Eu_2O_3/TiO_2.

3.1.2 The EDX and X- ray Diffraction of Eu_2O_3/TiO_2

The results of the EDX spectrum analysis of Eu_2O_3/TiO_2 confirmed the presence of Eu in the modified sample at approximately 5-7 keV. It demonstrated that the introduction of Eu_2O_3 to TiO_2 created denaturation causing the shift of the absorption spectrum region of TiO_2 towards the visible light.

X-ray diffraction diagram of Eu_2O_3/TiO_2 (Fig. 2), peaked at position 2^{θ}= 25.4°, 36.9°, 37.85°, 48.0°, 53.9°, 55.05°, 62.7°, and 68.8° characterizing the TiO_2 structure in the form of anatase.

This proves that the process of denaturing TiO_2 by Eu_2O_3 does not change the phase composition of the material. Besides the presence of TiO_2, peaks at position 22.9° appear to characterize the crystal structure of Eu_2O_3.

3.1.3 SEM and TEM Images

For photocatalytic materials, the particle size has a great influence on their catalytic capacity; the smaller the particle size, the greater the surface area and the higher the efficiency in receiving electrons from light.

The results of SEM and TEM scanning of the Eu_2O_3/TiO_2 (Fig. 3) showed that the surface structural

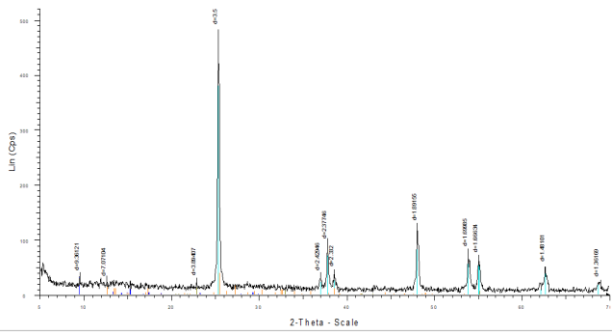

Fig. 2 X-ray diffraction diagram of Eu_2O_3/TiO_2.

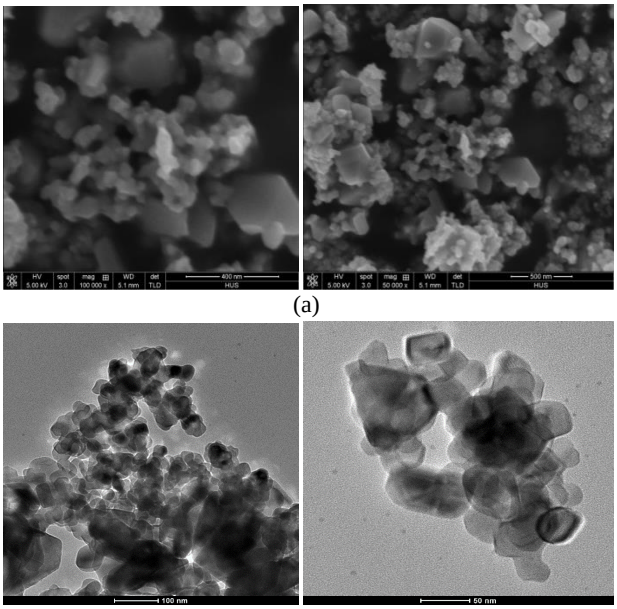

Fig. 3 SEM (a) and TEM (b) images of Eu_2O_3/TiO_2 nanostructures.

morphology of the material was relatively spongy, the particles were relatively uniform in size and they had a spherical shape arranged and evenly distributed alongside the TiO_2 nanoparticles. The average size of the particles was about 10-30 nm.

3.1.4 UV-VIS Spectrum

Comparision of UV-VIS spectral results among TiO_2; and Eu_2O_3/TiO_2 nanostructures (Fig. 4) showed that the TiO_2 nanostructure had a maximum absorption at 370 nm while the Eu_2O_3 nanostructure had maximum adsorption at 240 nm. In the case of the Eu_2O_3/TiO_2 mixed-oxide nanostructure, the maximum absorption of the UV-VIS spectrum transferred to the visible light region at 410-425 nm. This proved that the combination of Eu_2O_3 and TiO_2 had led to a shifting of the maximum absorption, expanding the forbidden band of TiO_2 towards the visible light.

3.2 Photocatalytic Active of Nano Eu_2O_3/TiO_2

3.2.1 Effect of Eu_2O_3/TiO_2 Ratios on Catalytic Activity of the Photocatalyst Degradation of MB

The effect of Eu_2O_3/TiO_2 ratios (w/w) on the catalytic activity were surveyed using different Eu_2O_3/TiO_2 ratios: 0/1, 1/5, 1/10, 1/15 and 1/20.

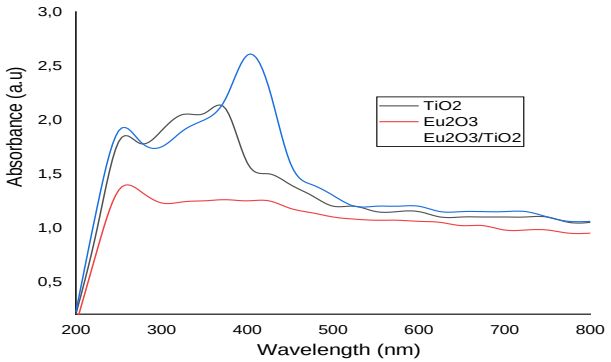

Fig. 4 UV-Vis adsorption spectra of TiO_2, Eu_2O_3 and Eu_2O_3/TiO_2.

Material synthesis conditions and MB treatment tests included the gel burning temperature (550°C). The amount of catalyst used was 0.05 g with the volume of 20 ppm MB solution (100 ml) for 2 hours at 70°C**,** under visible irradiation for all experiments.

The results are shown in Fig. 5. It showed that the TiO_2 nanocatalyst photocatalytic material had the lowest MB treatment efficiency. For Eu_2O_3/TiO_2 nanocatalytic materials with different Eu_2O_3/TiO_2 ratios, the MB treatment efficiency is much higher than that of the TiO_2 nanomaterial. At the rate of 1/15 and 1/10, the Eu_2O_3/TiO_2 materials had the best catalytic activity, MB efficiency reached about 90% after 2 hours.

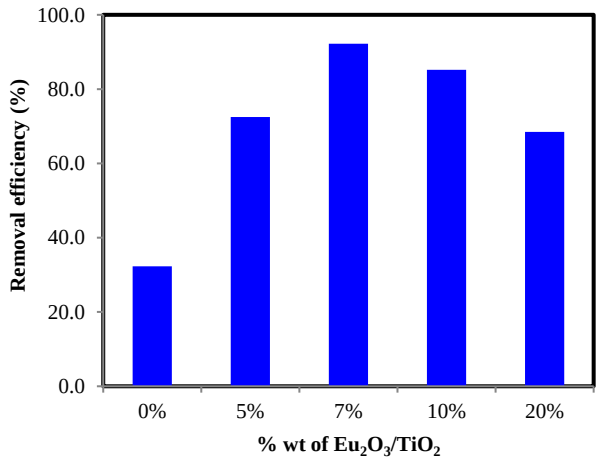

Fig. 5 Graph showing the effect of Eu_2O_3/TiO_2 to degradation of methylene blue in aqueous solutions under visible irradiation (Experimental conditions: V_{MB} =100 mL, C_o = 10 ppm, m: catalyst = 0.05 g, pH = 6, 2 hours, T = 70°C).

3.2.2 The Effect of Burning Temperature of Photocatalytic Synthesis Process on Methylene Blue Degradation

Based on the results of the above experiment and the results of other research on the fabrication of TiO_2 photocatalytic nanomaterial, the burning temperatures for synthesizing the catalyst were set at 450°C, 500°C, 550°C, and 600°C for 3 hours and the TiO_2/Eu_2O_3 ratio was 15/1. The effect of the burning temperature of catalyst synthesis process on MB oxidation capability is shown in Table 1.

From Table 1, we found that the burning temperature of 550°C gave the highest treatment efficiency at 92.7%. According to other studies, this is reasonable because at 550°C the TiO_2 is converted to anatase with the best photocatalytic activity compared to other crystalline polyforms, which was explained based on the energy band structure of TiO_2 nanomaterial [2, 3, 8, 9].

3.2.3 The Effect of pH

The pH of the solution is one of the important factors influencing process performance destroying many substrates in the photocatalytic process [28]. MB decomposition efficiency increased sharply, when pH increased from 3 to 5, partly stablized at pH from 4 to 8 but then decreased when the pH increased to 12 (see Fig. 6).

Some researchers suggested that the effect of pH on the photocatalytic decomposition process [26, 27] is very complicated. The results obtained above can be explained based on the surface charge of the object catalyst materials and pigments. Firstly, MB is the basic pigment existing in the form of clear cations in water with pKa = 3.8. When pH > 3.8, the surface of MB molecule is positively charged [28].

Table 1 Results of investigating the effect of baking temperature on Methylene blue degradation.

Heating temperature (°C)	450	500	550	600
Initial MB concentration C_o (ppm)	20	20	20	20
MB concentration after reaction Ct (ppm)	7.58	4.62	1.46	2.72
Conversion (%)	62.1	76.9	92.7	86.4

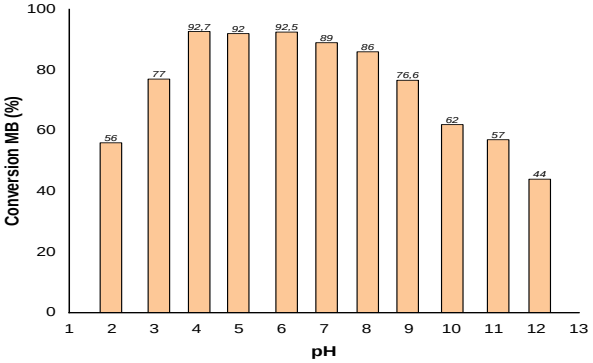

Fig. 6 Conversion of MB under visible irradiation at various pH (Experimental conditions: V_{MB} =100 mL, C_o = 20ppm, m: catalyst = 0.05 g Eu_2O_3/ TiO_2 = 1/15, 2 hours, T = 70°C).

Second, the value of pH_{PHC} isoelectric point of the Eu_2O_3/TiO_2 material according to this study has a value in the range of 4.12 ÷ 4.95, depending on the Eu_2O_3/TiO_2 ratio. At pH = 3 < pH_{PZC}, the surface of the material is positively charged due to the protonation process, while the MB fraction is not charged so the main interaction between the catalyst surface and the main coloring matter is a weak van der Waals interaction. It leads to very poor ability to adsorb MB on the catalyst surface, subsequentially causing the photochemical decomposition reaction to occur with very low efficiency. Moreover, the positive charge of the surface can limit the supply of hydroxyl ions needed to form free radicals that play an important role in the decomposition of pigments. When pH = 5 (greater than the pH_{PHC} value of the material as well as the pKa of MB), photochemical decomposition efficiency increased sharply due to electrostatic interaction between the surface of the negatively charged material (from proton separation) and positively charged MB cation dominateds. It resulted in a notable increase in adsorption and stronger photochemical reaction. MB decomposition efficiency continued to increase with increasing pH and reached a maximum of 92.7 % at pH = 6. However, when at pH > 8, photochemical degradation is inhibited by hydroxyl ions that compete with the internal MB fraction absorption on the surface of the catalyst. Thus, the MB

decomposition efficiency was decreased when pH increased more than 8.

3.2.4 The Effects of Reaction Temperature

The effect of times on the oxidative desulfurization of MB during visible irradiations is shown in Fig. 7. After 2 h, the deep desulfurization could be achieved with 40% conversions at 30°C; 59.6% at 50°C and 92.2% at 70°C under visible light irradiation respectively. The results are in good agreement with the literature where an increase in the reaction temperature improved the photodegradation efficiency [25].

3.2.5 The Evaluation of Photocatalytic Activity of Eu_2O_3/TiO_2 Photocatalyst Under Dark, Visible and UV Irradiation

For comparison, the degradation of MB over Eu_2O_3/TiO_2 by the irradiation of UV, visible light and dark was carried out at 70°C and various times, where MB concentration was 20 ppm, pH = 4.

The results in Fig. 8 show that the photocatalytic activities of the Eu_2O_3/TiO_2 material under different light conditions are different. In the absence of illumination (darkness) the MB oxidation efficiency of the material is low; only 15.4% conversion after 2 hours. The reduced amount of MB is expected to be due to the adsorption process. Under UV and visible light conditions, MB convension reached 74.2% and 80.7% after 2 hours. The results again demonstrated that there is a shift of the band gap of Eu_2O_3/TiO_2 material toward the visible light region, which increases the photocatalytic activity of the material.

3.2.6 Reaction Kinetics

For further study, to compare the decomposition reaction rate of Eu_2O_3/TiO_2 materials with different ratios, the Langmuir-Hinshelwood kinematic model was used. The result is shown in Fig. 9.

The decomposition reaction kinetics of MB: Fig. 9 shows the relationship of ln (C_o/C_t) with reaction time (t) is linear. This shows that the catalytic reaction follows the Langmuir-Hinshelwood kinematic model and is a simple first order reaction, with a high

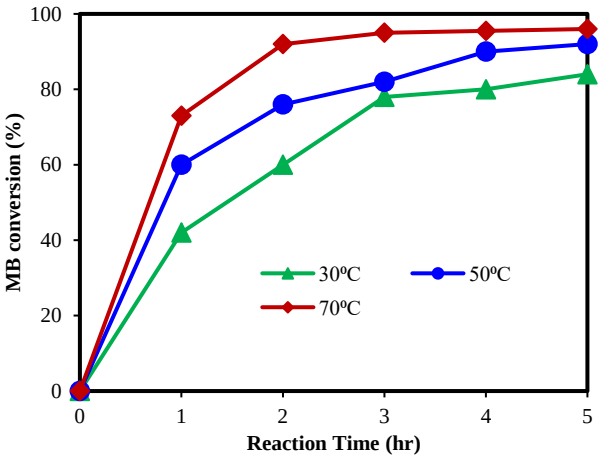

Fig. 7 Conversion of MB under visible irradiation at various time (Experimental conditions: V_{MB} =100 mL, C_o = 20ppm, m: catalyst = 0.05 g Eu_2O_3/ TiO_2 = 1/15, pH = 4).

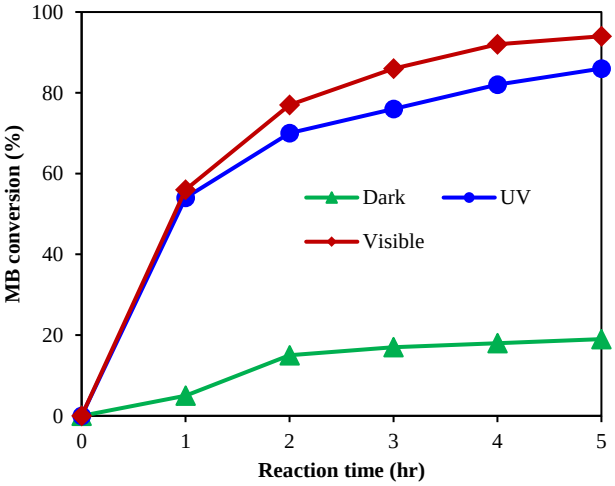

Fig. 8 Conversion of MB under irradiation of UV, visible light anh dark at various time (Experimental conditions: V_{MB} = 100 mL, C_o = 20 ppm, m: catalyst = 0.05 g Eu_2O_3/ TiO_2 = 1/15, pH = 4, T = 70°C).

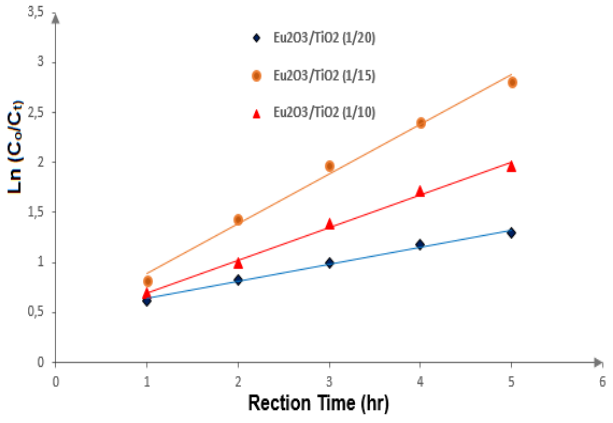

Fig. 9 The relationship between ln (C_o/C_t).

correlation coefficient ($R^2 \geq 0.99$). From this relationship, kapp values and regression coefficients were calculated (Table 2). The decomposition reaction kinetics of MB Fig. 9 shows the relationship of $\ln(C_o/C_t)$ and the reaction time (t) was linear. This shows that the catalytic reaction follows the Langmuir-Hinshelwood kinematic model and is a simple first order reaction, with a high correlation coefficient ($R^2 \geq 0.99$). From this relationship, kapp values and regression coefficients were calculated (Table 2).

Photocatalytic activity of the samples decreased in the Eu_2O_3/TiO_2 (1/20) ratio < Eu_2O_3/TiO_2 (1/10) < Eu_2O_3/TiO_2 (1/15). Especially for the Eu_2O_3/TiO_2 (1/15) samples, the MB decomposition rate was 2.9 times higher than the Eu_2O_3/TiO_2 (1/20) samples. It is shown that the ratio of Eu_2O_3 to TiO_2 plays an important role in affecting the crystal lattice structure of TiO_2, as well as the overall photocatalytic activity of Eu_2O_3/TiO_2 materials.

Table 2 Result of Kinetic investigating based on the Langmuir-Hinshelwood model.

Materials	Equation	K_{app} ($hour^{-1}$)	Correlation coefficient R^2
Eu_2O_3/TiO_2 (1/15)	Y= 0.4966x + 0.3974	0.496	0.992
Eu_2O_3/TiO_2 (1/10)	Y= 0.3266x + 0.371	0.326	0.995
Eu_2O_3/TiO_2 (1/20)	Y= 0.171x + 0.4678	0.171	0.990

4. Conclusion

In summary, the photocatalytic of nano Eu_2O_3/TiO_2 has been successfully synthesized using oxide of Eu_2O_3 and tetra-n-butyl orthotitanate by the sol gel method. The obtained results on the fabrication of Eu_2O_3/TiO_2 mixed-oxide photocatalysts revealed that the average size of the catalyst particles was in the range of 10-30 nm. The synthesized Eu_2O_3/TiO_2 at a ratio of 1/15 exhibited the best photocatalytic activity in MB degradation in an aqueous solution under visible irradiation. The photocatalyst system was capable of decomposing 92.7% of MB (concentration 20 ppm) in aqueous solutions after 2 hours at 70°C. The results of this study will contribute to the improvement of the use of modified TiO_2 photocatalytic materials in environmental remediation, especially the degradation of methylene blue in aqueous solutions.

Acknowledgement

This research was funded by the Hanoi University of Natural Resources and Environment, Vietnam.

References

[1] D. Wu and M. Long, Low-temperature synthesis of N-TiO_2 sol and characterization of N-TiO_2 coating on cotton, fabrics, *Surface & Coatings Technology* 206 (2012) 3196-3200.

[2] C. P. Lin, H. Chen, A. Nakaruk, P. Koshy and C. C. Sorrell, Effects of annealing temperature on the photocatalytic activity of N-doped TiO_2 thin film, *Energy Procedia* 34 (2013) 627-636.

[3] T. Tachikawa, M. Fujitsuka and M. T. Majima, Mechanistic insight into the TiO_2 photocatalytic reactions: design of new photocatalysts, *J. Phys. Chem.* 111 (2007) (14) 5259-5275.

[4] Z. Teng, X. Su, G. Chen, C. Tian, H. Li and L. Ai, Superparamagnetic high-magnetization composite microspheres with Fe_3O_4@SiO_2 core and highly crystallized mesoporous TiO_2 shell, *Colloid and Surface A: Physicochem, Engineer, Aspects* 402 (2012) 60-65.

[5] H. Diker, C. Varlikli, K. Mizrak and A. Dana, Characterizations and photocatalytic activity comparisons of N-doped ncTiO_2 depending on synthetic conditions and structural differences of amine sources, *Energy* 36 (2011) 1243-1254.

[6] Feng, Europium-containing nanoparticle material useful for solar and thermal energy conversion and related uses, WIPO Patent Application, 2007, WO/2007/130671.

[7] B. Liang and M. X. Zhu, Synthesis and photoluminescence of new europium complex Eu(DBM)3(DPPZ) with dipyridophenazine ligand, *Chinese Chemical Letters* 14 (2003) (1) 43-46.

[8] W. Shipeng and Z. Xiaoping, Fluorescence and Judd-Ofelt analysis of rare earth complexes with maleic anhydride and acrylic acid, *Journal of Rare Earths* 26 (2008) (6) 787-791.

[9] C. Yang, Z. Feng Sun, L. Liu and L. Q. Zhang, Preparation and luminescence performance of rare earth agriculture-used light transformation composites, *J. of*

Materials Sci. 43 (2008) (5) 1681-1687.

[10] Z. Zhang, C. Zhang, M. Fan and W. Yan, Synthesis and complexation mechanism of europium ion (Eu^{3+}) with spiro[indoline-phenanthrolineoxazine, *Dyes and Pigments* 77 (2) (2008) 469-473.

[11] S. Yin, M. Shinozaki and T. Sato, Synthesis and characterization of wire-like and near-spherical Eu_2O_3-doped Y_2O_3 phosphors by solvothermal reaction, *J. Lumin.* 126 (2007) 427-433.

[12] H. Hu, W. J. Xiao, J. Yuan, J. W. Shi, M. X. Chen and W. F. Shang Guan, High photocatalytic activity and stability for decomposition of gaseous acetaldehyde on TiO2/Al2O3 composite films coated on foam nickel substrates by sol-gel processes, *J. Environ. Sci.* 19 (2007) (1) 80-85.

[13] S. Y. Lee and S. J. Park. "TiO2 photocatalyst for water treatment application". J. Indus. Eng. Chem., Vol 19 (6) (2013), pp 1761–1769.

[14] M. A. Kebede, M. E. Varner, N. K. Scharko, R. B. Gerber and J. D. Raff, Photooxidation of ammonia on TiO_2 as a source of NO and NO_2 under atmospheric conditions, *J. of the American Chem. Society* 135(2013) (23) 8606-8615.

[15] Q. Zhang, J. B. Joo, Z. Lu, M. Dahl, D. Q. L. Oliveira, M. Ye and Y. Yin, Self-assembly and photocatalysis of mesoporous TiO_2 nanocrystal clusters, *Nano Research* 4 (2011) (1) 103-114.

[16] S. Son, S. H. Hwang, C. Kim, J. Y. Yun and J. Jang. Designed synthesis of SiO_2/TiO_2 core/shell structure as light scattering material for highly efficient dye-sensitized solar cells, *ACS Applied Materials and Interfaces* 5 (2013) (110) 4815-4820.

[17] H. Lachheb, O. Ahmed, A. Houas and J. P. Nogier, Photocatalytic activity of TiO_2-SBA-15 under UV and visible light, *J. of Photochem. Photobio. A: Chemistry* 226 (2011) (1) 1-8.

[18] T. Kamegawa, Y. Ishiguro, R. Kido and H. Yamashita, Design of composite photocatalyst of TiO_2 and Y-zeolite for degradation of 2-propanol in the gas phase under UV and visible light irradiation, *Molecules* 19 (2014) (10) 16477-16488.

[19] A. Crake, K. C. Christoforidis, A. Kafizas, S. Zafeiratos and C. Petit, CO_2 capture and photocatalytic reduction using 8 Journal of Chemistry Bifunctional TiO_2/MOF nanocomposites under UV–vis irradiation, *Applied Catalysis B: Environmental* 210 (2017) 131-140.

[20] Y. Zhang, T. Wang, M. Zhou, Y. Wang and Z. Zhang, Hydrothermal preparation of Ag-TiO_2 nanostructures with exposed facets for enhancing visible light photocatalytic activity, *Ceramics International* 43 (2017) (3) 3118-3126.

[21] L. Xu, E. M. P. Steinmiller and S. E. Skrabalak, Archieving synergy with a potential photocatalytic Z-scheme: Synthesis and evaluation of nitrogen-doped TiO_2/SnO_2 composites, *J. of Physical Chemistry* 116 (2012) (1) 871-877.

[22] D. Lu, S. Ouyang, H. Xu, D. Li, X. Zhang and Y. Li, Designing A surface-modified nanoporous-single-crystalline $SrTiO_3$ to optimize diffusion of surface plasmon resonanceinduce photoelectron toward enhanced visible-light photoactivity, *ACS Appl. Material Interfaces* 8 (2016) (14) 9506-9513.

[23] J. G. Santos, J. D. L. Dutra, S. Alves Jr., R. O. Freire and N. B. da Costa Jr, Theoretical Spectroscopic Study of Europium Tris(bipyridine) Cryptates, *J. Phys. Chem. A* 116 (2012) 4318-4322.

[24] R. S. Viana, E. H. L. Falcao, J. D. L. Dutra, N. B. Costa Jr, R. O. Freire and S. Alves Jr, New experimental and theoretical approach in Eu_2O_3 microspheres: from synthesis to a study of the energy transfer", *J. of Photochem and Photobio. A Chemistry* 281 (2014) 1-7.

[25] N. A. M. Barakat, M. A. Kanjwal, I. S. Chronakis and H. Y. Kim, Influence of temperature on the photodegradation process using Ag-doped TiO_2 nanostructures: Negative impact with the nanofibers, *J. of Molecular Catalysis A: Chemical* 366 (2013) 333-340.

[26] J. Sun, Y. Wang, R. Sun and S. Dong, Photodegradation of azo dye Congo Red from aqueous solution by the WO_3–TiO_2/activated carbon (AC) photocatalyst under the UV irradiation, *Materials Chem. and Phys.* 115 (2009) (1) 303-308.

[27] M. Panizza and M. A. Oturan, Degradation of Alizarin Red by electro-Fenton process using a graphite-felt cathode, *Electrochimica Acta.* 56 (2011) (20) 7084-7087.

[28] J. Saien and S. Khezrianjoo, Degradation of the fungicide carbendazim in aqueous solutions with UV/TiO_2 process: Optimization, kinetics and toxicity studies, *J. of Hazardous Materials* 157 (2008) (2-3) 269-276.

[29] N. N. Dao and M. D. Luu, Synthesis and investigation on CO catalytic oxidation of Ce0, 5Zr0, 5O2 prepared by combustion method using polyvinyl alcohol, *Advances in Natural Sciences: Nanoscience and Nanotechnology* 14 (2012) (3) 015014.